

A New Ti:Sapphire Laser System: A Source of Femtosecond Pulses Tunable from Ultraviolet to Infrared

The availability of reliable, solid-state laser sources that produce femtosecond pulses with energies of about 1 mJ and repetition rates of 1 kHz provides new prospects for ultrafast laser spectroscopy. The Ti:sapphire oscillator/amplifier system is such a source. Nonlinear optical conversion of its output frequency using optical parametric generation/amplification or sum and difference frequency mixing effectively extends the spectral range available for femtosecond optical experiments. At LLE/COI, several UR faculty members are working to produce a multiuser laser system that will generate femtosecond pulses tunable through the visible and a large portion of the infrared. Such a system will be used for experiments in materials research, nonlinear optics, atomic and plasma physics, electronic devices, and circuits testing. In this article we describe the layout of the system under development, the main components and their characteristics, and the applications of the system. We also present the first experimental results produced at this facility.

System Configuration

A Ti:sapphire oscillator/chirped-pulse-amplification system—comprising an oscillator, stretcher, regenerative amplifier, and compressor—is the source of sub-100-fs pulses in the

800-nm spectral range with 1- to 5-kHz repetition rate. Figure 65.42 shows the layout of this system. The amplifier output is used to pump three devices: a white-light continuum generator (WLC), an optical parametric amplifier (OPA), and a terahertz (THz) radiation source. The continuum generator produces femtosecond pulses in the visible and near-infrared. Its output may serve as both a probe beam in ultrafast pump-probe experiments and a seed for the optical parametric amplifier. The output of the OPA lies in the near-infrared range ($\lambda = 1.2$ to $2.4 \mu\text{m}$). The signal and idler waves out of the OPA are mixed in the difference frequency generator (DFG), producing tunable femtosecond pulses in the mid-infrared range (up to $12 \mu\text{m}$ and possibly longer wavelengths). The output of Ti:sapphire oscillator also pumps the optical parametric oscillator (OPO) that produces signal and idler waves covering the range between 1.35 and $2.0 \mu\text{m}$. The OPO output can also be mixed in a difference frequency generator giving femtosecond pulses in the mid-infrared range at a repetition rate of 82 MHz.

Ti:Sapphire Oscillator/Amplifier

The core of this system is a Ti:sapphire oscillator/amplifier combination manufactured by Spectra Physics Lasers in collaboration with Positive Light. The oscillator is a regeneratively

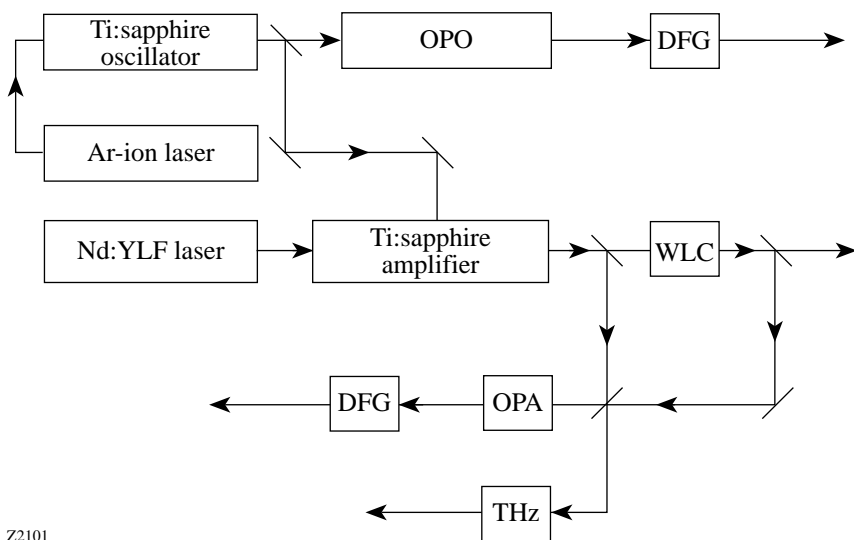


Figure 65.42
General layout of the femtosecond Ti:sapphire-based laser system. OPO—optical parametric oscillator; OPA—optical parametric amplifier; WLC—white-light continuum generator; DFG—difference frequency generator; THz—terahertz radiation generator.

Z2101

mode-locked Tsunami (model 3960),¹ pumped by 8 to 12 W from an Ar-ion laser, and produces pulses at 82-MHz repetition rate. Typical pulse duration at the laser output is 70 to 80 fs, but, using an external prism compressor, pulses as short as 45 fs can be obtained [Fig. 65.43(a)]. The spectral width (FWHM) of the oscillator output is typically 15 to 17 nm [Fig. 65.43(b)]. Currently, the Tsunami tuning range is 720 to 850 nm and the output power is about 1 W. To pump the optical parametric oscillator, which requires higher pump power levels, the Ti:sapphire oscillator cavity is reconfigured to deliver up to 2 W of average power and slightly longer pulses (90 to 100 fs).

Part of the Ti:sapphire oscillator output is split off to seed the amplifier—a Spitfire, from Spectra Physics Lasers and Positive Light. The amplifier utilizes the chirped-pulse-amplification technique,² where the seed pulses are first stretched to about 150 ps in a diffraction-grating stretcher to reduce nonlinear effects and avoid damage to the optical elements in the amplifier and, at the same time, to allow efficient energy extraction from the amplifier. These temporally expanded pulses are switched into a regenerative amplifier cavity. The Ti:sapphire amplifier is pumped by a Nd:YLF *Q*-switched laser (Merlin, from Spectra Physics Lasers and Positive Light), which is capable of producing up to 12 W of average power at 527 nm (200- to 300-ns pulses at 1 kHz). After 15 to 20 round-trips through the amplifier cavity, amplified pulses are switched out and contain 1 to 1.5 mJ per pulse (the repetition rate is that of the pump laser—1 kHz). Following this amplification, the pulses are compressed to 75 to 140 fs in the diffraction-grating compressor [Fig. 65.43(a)], depending on the seed pulses' characteristics. The energy per pulse is up to 1 mJ at 1-kHz repetition rate (i.e., 1-W average power) when operating near

800 nm with a pulse-to-pulse energy stability of ~2%. The amplifier is also capable of higher repetition rates—up to 5 kHz, producing up to 1.5 W of average power.

White-Light Generator

To perform time-resolved spectroscopic measurements (pump-probe experiments) in a broad spectral range, we utilize the technique of femtosecond continuum (or supercontinuum) generation. Femtosecond pulses out of the Ti:sapphire amplifier are focused onto a plate of glass or crystalline material. For pump intensities above a certain threshold, broadband radiation spanning the entire visible and a portion of near-infrared range is produced at the output of the plate. A number of mechanisms are involved in continuum generation, the major being spectral broadening of the pulses due to self-phase modulation.³ The generation of femtosecond continuum requires materials with a high nonlinear refractive index and resistance to damage at very high intensities. We tested a number of glass and crystalline materials and, based on a compromise between efficient continuum generation in the near-infrared and resistance to optical damage, we selected BaF₂ crystals. The threshold for continuum generation in a BaF₂ plate of 5-mm thickness was about 1 to 2 μ J per pulse (the pump radiation was focused onto the crystal using 20-cm-focal-length lens). Using a Si or Ge photodiode for detection, we observed continuum radiation spanning 400 nm to 1500 nm. Femtosecond continuum was also generated using the second harmonic ($\lambda = 400$ nm) of a Ti:sapphire system; the output is in the visible-ultraviolet spectral range. For the pump-probe measurements, portions of the continuum in the spectral range of interest are selected using bandpass interference filters. The duration of probe pulses produced in this manner is nearly that of the pump pulses (~100 fs).

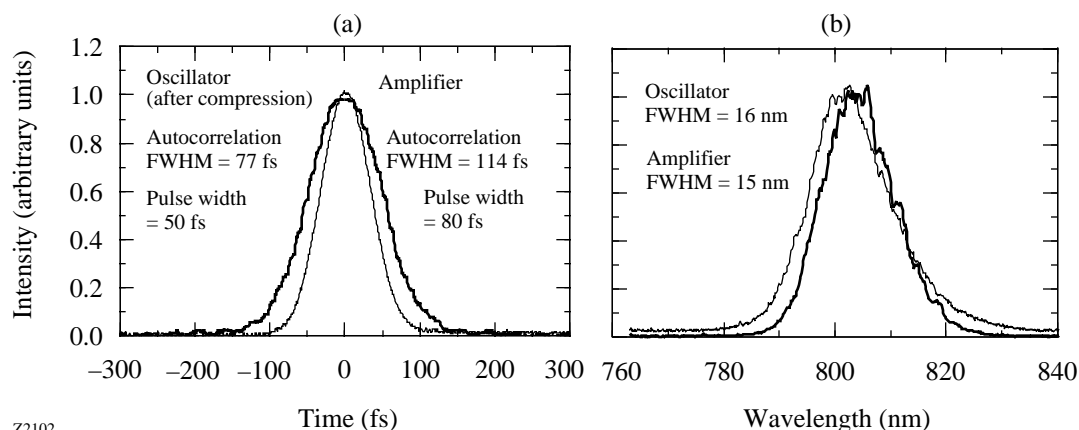


Figure 65.43

(a) Intensity autocorrelation functions and (b) spectra of the Ti:sapphire oscillator (thin line) and regenerative amplifier (thick line).

Z2102

Although it is easy to implement, femtosecond continuum generation over a broad spectral range has certain limitations. First, the intensity of the continuum drops rapidly when moving away from the pump wavelength. The useful spectral range in the infrared is limited to 1.3 to 1.5 μm when pumped by pulses centered at 800 nm. Second, the intensity of the continuum may be too low for many applications. To produce intense, tunable femtosecond pulses in a broad spectral range, we use the optical parametric amplification technique and subsequent difference frequency mixing.

Optical Parametric Amplifier and Difference Frequency Generator

To generate femtosecond pulses in the 1.2- to 2.5- μm range we are developing a traveling-wave optical parametric amplifier that is seeded by pulses from the white-light continuum generator.⁴ Seeding the OPA with femtosecond continuum pulses allows operation at lower pump levels (as compared to the optical parametric generator/amplifier configuration, which utilizes parametric fluorescence as the seed) and leads to more reliable and stable operation. Our OPA is based on a BBO crystal, which combines high second-order nonlinearity and high damage threshold. In the first experiment, we used a 7-mm-thick BBO crystal cut for type-II phase matching to reduce the bandwidth of the OPA output and to generate pulses that are closer to the transform limit than in the case of type-I phase matching. This also provides signal and idler waves of orthogonal polarizations that are convenient for subsequent difference frequency mixing. (Phase matching in a AgGaS_2 difference frequency generator requires orthogonally polar-

ized input waves.) The layout of the two-pass, single-crystal OPA is shown in Fig. 65.44. The output of the white-light continuum generator and the pump radiation at 810 nm are collinearly combined in the nonlinear crystal using a dichroic mirror. The white-light seed is not spectrally filtered before the OPA since the nonlinear crystal, with its limited wavelength acceptance bandwidth, is a natural spectral filter. The central wavelength is selected by angular tuning of the OPA crystal. The first-pass OPA output is backreflected onto the crystal and is again combined collinearly with a fresh portion of the 800-nm pump using a dichroic mirror. The temporal overlap between the pump and seed (first pass), and the pump and the signal wave (second pass) is adjusted by two optical delay lines. When 100- μJ pulses were used to pump the first pass and 200 μJ for the second pass, the OPA output was more than 40 μJ per pulse (total output in signal and idler beams). Figure 65.45 is a demonstration of the tunability from degeneracy down to 1.2 μm (signal wave) and up to 2.4 μm (idler). The spectral width of the OPA output is about 25 nm FWHM (signal wave), which is enough to support pulses shorter than 100 fs. In the first experiments, the pump-pulse duration was 140 fs, and measurements of the cross correlation between the OPA output and the pump pulses indicated an OPA output pulse duration of about 200 fs. The excessive pulsewidth of the OPA output is most likely a result of a group-velocity mismatch between the interacting waves. For three-wave type-II interaction in BBO the group-velocity mismatch is calculated, using Sellmeier equations,⁵ to be about 80 fs/mm. The crystal length in our OPA should, therefore, be reduced to optimize performance.

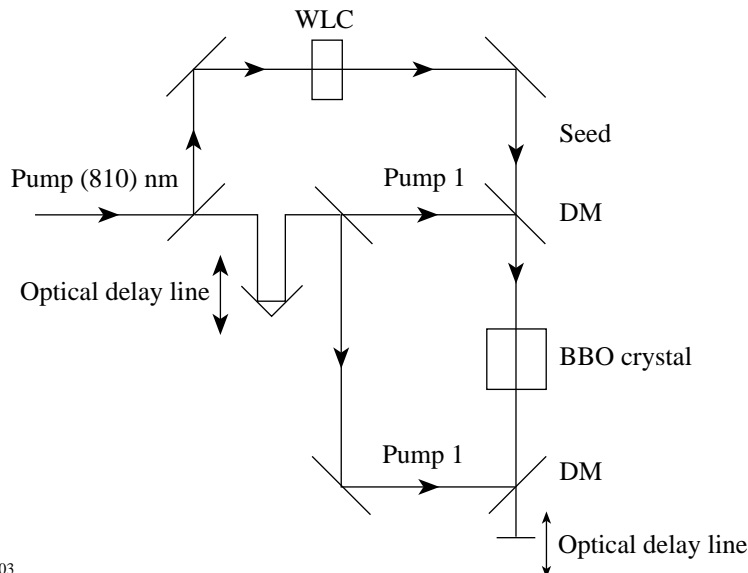


Figure 65.44
Optical parametric amplifier layout. WLC—white-light continuum generator; DM—dichroic mirror.

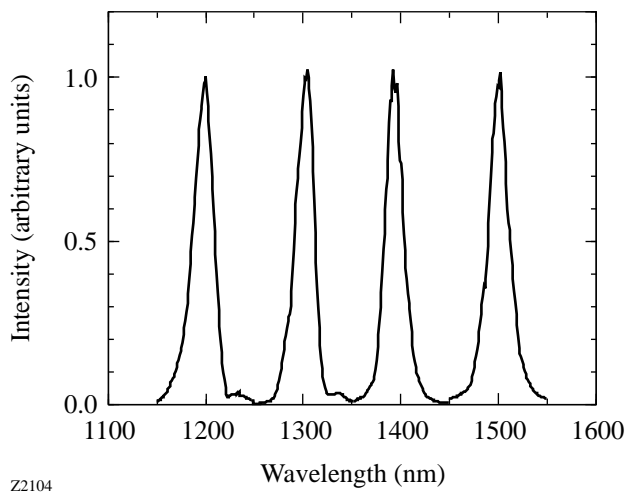


Figure 65.45
The spectrum of the OPA output.

To generate femtosecond pulses in the mid-infrared range, the signal and idler waves from the OPA are mixed in a difference frequency generator (Fig. 65.46 shows the expected tuning range of the DFG). A 1-mm-thick AgGaS_2 crystal, which is transparent up to $12\ \mu\text{m}$, was used for difference frequency mixing. With $30\ \mu\text{J}$ per pulse input (signal and idler) more than $300\ \text{nJ}$ per pulse was obtained at $5\text{-}\mu\text{m}$ wavelength. The spectral width of the mid-infrared pulses was about $200\ \text{nm}$ —sufficient to produce pulses as short as $130\ \text{fs}$.

It is worth mentioning that the OPA output pulses are of sufficient energy to generate femtosecond continuum in solid-state media. This continuum can be a broadband source of femtosecond pulses in the near- and mid-infrared that presents new possibilities for ultrafast spectroscopy in this range.

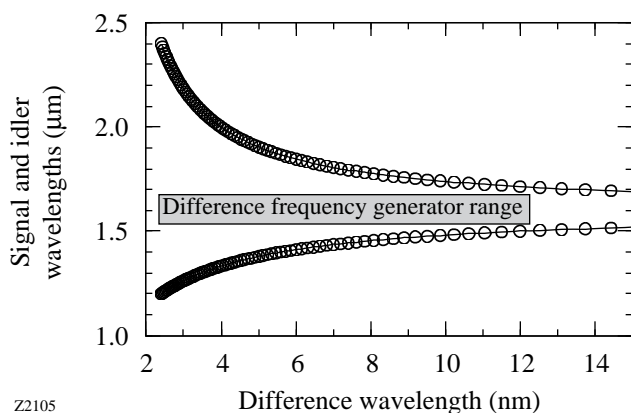


Figure 65.46
Tuning range of a difference frequency generator pumped by the OPA output.

The demonstrated performance of the OPA and DFG has already allowed several interesting time-resolved experiments to be performed in the near- and mid-infrared ranges. Work continues on the optimization of conversion efficiency and pulse durations.

Optical Parametric Oscillator

Femtosecond pulses in the near-infrared region at a high repetition rate ($82\ \text{MHz}$) can be produced using a synchronously pumped optical parametric oscillator—OPAL, manufactured by Spectra-Physics Lasers. The OPAL is based on a temperature-tuned noncritically phase-matched LBO crystal and is capable of delivering pulses of about 100-fs duration in the spectral range of 1.35 to $1.6\ \mu\text{m}$ (signal wave) and 1.6 to $2.0\ \mu\text{m}$ (idler wave). (The wavelength is determined by the spectral characteristics of the OPAL cavity mirrors.) When pumped by about $2\ \text{W}$ of average power from a Ti:sapphire oscillator, the OPAL produces an output of more than $250\ \text{mW}$ (signal) and about $150\ \text{mW}$ (idler) at the maximum of its tuning curve (signal wave at around 1.45 to $1.50\ \mu\text{m}$). A typical spectrum and an autocorrelation function of the OPAL output are shown in Fig. 65.47.

Mixing the signal and idler beams in the difference frequency generator can produce mid-infrared femtosecond pulses from 4 to $12\ \mu\text{m}$. Using a 1-mm -thick AgGaS_2 crystal for difference frequency mixing, up to $50\ \mu\text{W}$ of average power was generated in the 4- to $10\text{-}\mu\text{m}$ range. In this range, group-velocity mismatch between interacting waves (signal, idler, and difference) in AgGaS_2 does not exceed $200\ \text{fs/mm}$, so the difference frequency pulses out of the 1-mm -thick crystal should not be longer than $200\ \text{fs}$ when the input signal and idler pulses are $100\ \text{fs}$ long.

THz Radiation Generator

Work is currently underway to produce ultrashort pulses of terahertz radiation (the sub-millimeter range of the spectrum). A high-power source of terahertz radiation, called a large-aperture photoconducting antenna,^{6,7} consists of a 6-cm^2 GaAs wafer that is biased using parallel electrodes spaced $2\ \text{cm}$ apart. Semi-insulating GaAs is used to hold off a bias voltage of $10\ \text{kV}$. When a high-energy Ti:sapphire pulse uniformly illuminates the antenna, electrons are excited into the conduction band and the antenna becomes conductive. The sharp turn-on of surface current produces radiation that is polarized along the bias-field direction. In the far field, the radiated electric field is proportional to the rate of change of the surface current, the bias field, and the energy of the optical

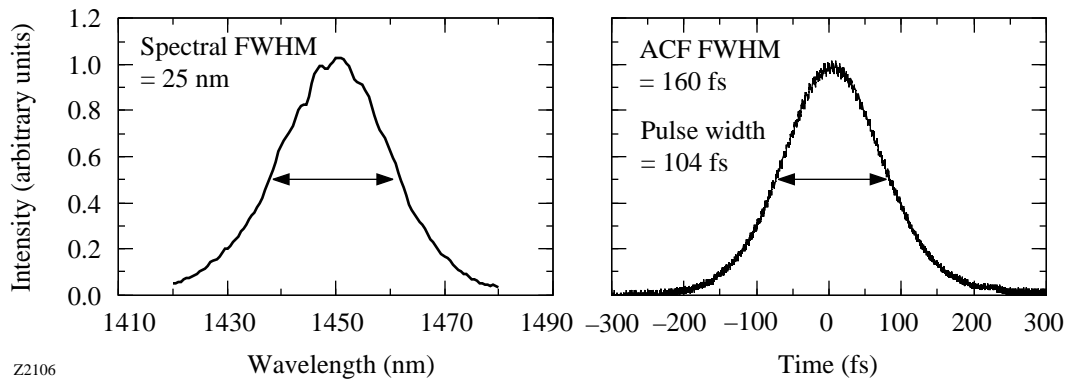


Figure 65.47
Spectrum and intensity autocorrelation function of the OPAL output pulses (signal wave).

Z2106

pulse. The large-aperture design permits the use of high bias voltages and optical powers without damaging the antenna.

The THz radiation from this source is in the form of a beam of subpicosecond pulses. A 100-fs, 400-mJ Ti:sapphire pulse can produce a 450-fs, 0.8-mJ THz pulse.⁶ The unique feature of these THz pulses is that the pulse duration is less than the period of the electric field oscillation. Thus, it does not have a carrier wave in the usual sense. For this reason the pulses are sometimes referred to as dc pulses or half-cycle pulses.⁸

The short-term goal is to measure the spatial and temporal characteristics of such THz pulses. Of particular interest are the effects of diffraction and focusing on the pulse shape, and improvement of the shot-to-shot noise when the antenna is saturated. A variety of techniques will be used to do this. Initially, the temporal profile of the pulses will be studied by passing the THz beam through a time-gated mirror and measuring the transmitted or reflected energy. The mirror consists of a second GaAs wafer that is illuminated by a delayed Ti:sapphire pulse.^{6,9} After absorption of the Ti:sapphire pulse, the transmission of a GaAs wafer at THz frequencies can be reduced by a factor of ten.⁶ Next, the power spectrum of the pulse will be measured using interferometric autocorrelation.⁹ Finally, electro-optic sampling techniques¹⁰ can be extended to freely propagating THz radiation to provide temporal and spatial information about the beam.

Once the nature of the THz pulses is better understood, work will begin on the long-term goal: the use of the THz pulses to manipulate the valence electron of a hydrogen-like atom. This type source has been used in atomic physics experiments to probe the electronic motion of highly excited (Rydberg) atoms.⁸ When the duration of a directional THz pulse is

shorter than the time scale of the electrons evolution, interaction between the THz pulse and an electron depends strongly on the shape of the electron wave function and its velocity. Furthermore, the large bandwidth of THz pulses enables electronic Rydberg states to be coherently coupled to neighboring states. These features may allow the use the THz pulses to excite and detect a three dimensionally localized Rydberg wave packet, which follows a circular orbit.¹¹

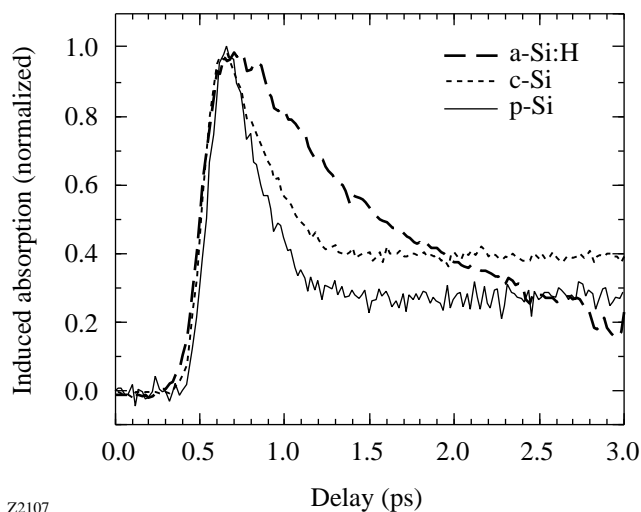
Initial Applications of the System

Using the pulses from the Ti:sapphire amplifier and the femtosecond continuum generator, pump-probe transient-absorption measurements were performed to better understand relaxation processes in silicon-based materials, low-temperature-grown A_3B_5 semiconductors, and polymers. Here the results of these measurements are briefly described.

The first experiments were performed on porous silicon, which has attracted significant attention since the 1990 discovery of its efficient light emission.¹² Normally, crystalline silicon does not emit light since it is an indirect band-gap material, but porous silicon, formed by electrochemical etching of crystalline silicon, luminesces effectively. Photoluminescence in the blue through near infrared has been observed, and light-emitting devices have been demonstrated.¹³ However, the energy structure of porous silicon and the origin of its efficient luminescence are still under debate. Time-resolved photoinduced absorption measurements (on a femtosecond scale) can be useful in clarifying the energy structure, determining the carrier relaxation mechanisms, and identifying the role of quantum confinement and defect states in porous silicon. Toward this end, pump-probe measurements on porous silicon, crystalline silicon (c-Si), and hydrogenated amorphous silicon (a-Si:H) samples have been conducted.

The porous Si sample was a 1- μm -thick mesoporous film lifted off and attached to a sapphire window. The c-Si sample was epitaxially grown on sapphire and was 530 nm thick. The a-Si:H sample was deposited on a glass window by RF glow discharge and was 320 nm thick. For these experiments, amplified Ti:sapphire pulses were frequency doubled to 3.06 eV (405 nm) to allow excitation of carriers across the band gap in the investigated samples. The probe was a portion of the white-light continuum, selected by a bandpass filter, and had a mean photon energy of 1.43 eV (870 nm).

Figure 65.48 shows the typical photoinduced absorption changes in the three samples. The traces for the porous Si and c-Si samples are similar to each other: both exhibit the increase in absorption when excited by 405-nm pulses; a short-lived (less than 1-ps decay constant) induced absorption peak decays into a "plateau." Longer time scans show that this plateau decays in hundreds of picoseconds. The initial peak is consistent with two-photon absorption—the simultaneous absorption of a pump and a probe photon across the direct band gap of silicon. The plateau in the induced absorption results from free-carrier absorption. That the dominant effect is induced absorption (as opposed to bleaching) is an indication of the indirect-band structure of porous silicon; in direct-gap semiconductors the dominant effect in the spectral range above the band gap is bleaching related to the filling of states. Based on our experimental results, we also estimated the free-carrier absorption cross section for the three silicon-based materials.



Z2107

Figure 65.48
Time-resolved photoinduced absorption in porous, crystalline, and amorphous Si.

The cross-section for porous Si ($1.2 \times 10^{-18} \text{ cm}^2$) is close to that of crystalline Si ($2.2 \times 10^{-18} \text{ cm}^2$) and much smaller than that of amorphous Si ($8 \times 10^{-17} \text{ cm}^2$). This is evidence that porous Si is made of an ordered lattice of Si atoms. By varying the excitation intensity we observed changes in the induced absorption decay rate. In porous silicon, the rapid decay (less than 1.5-ps lifetime) of the photoinduced free-carrier absorption was observed. Its time constant, which is nearly pulsewidth limited at low intensity, increases to about 1.5 ps as the pump intensity is increased. In porous silicon, this fast component probably originates from photoinjected carrier trapping by dangling bonds at the surface of silicon crystallites. Reduction of its decay rate is due to the saturation of the surface trapping states. These measurements show that trap saturation takes place at an injected carrier density of about 10^{18} cm^{-3} . The "slowly" decaying component of the induced absorption signal is due to carrier recombination through nonradiative Auger processes. The Auger mechanism of recombination is evidenced by the characteristic speeding up of the final stage of the absorption recovery when the pump intensity is increased.¹⁴

These initial photoinduced absorption experiments with the Ti:sapphire laser system provided information about the energy structure of porous silicon and carrier relaxation mechanisms in that material.

Another set of measurements was performed with GaAs grown by molecular-beam epitaxy at low substrate temperatures. Low-temperature (LT)-grown A_3B_5 semiconductors have recently attracted considerable interest due to their extremely rapid optical response times (several picoseconds). Initially, this fast response was attributed to carrier recombination. Pump-probe transient absorption experiments were performed at or below the band edge of GaAs samples grown at 195°C and 250°C to check the origin of this fast response time. The pump beam wavelength was 810 nm (1.531 eV), and the probe was varied from 870 nm (1.425 eV) to 1000 nm (1.24 eV).

The 250°C sample, which behaves very much like a normally grown GaAs, exhibits bleaching in the investigated spectral range. This bleaching may be attributed to the filling of bandtail states associated with defects due to low-temperature growth. On the other hand, the 195°C sample shows initial bleaching, which recovers quickly when the probe wavelength is in the vicinity of the band edge. When the probe is tuned to longer wavelengths (>900 nm), the signal changes to induced absorption with a relative slow recovery. The slowly recovering induced absorption shows that the carriers are trapped in

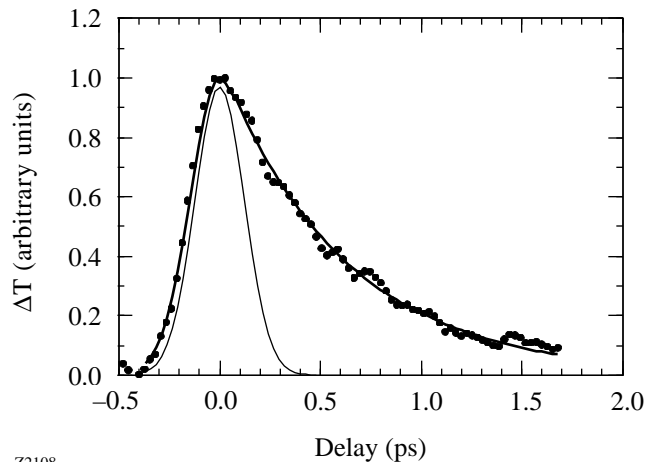
states below the band gap within several picoseconds but stay there for a long time until they recombine. This indicates that the observed fast, above-the-band-gap photoresponse time is due to carrier trapping, not recombination.

The same pump-probe technique with femtosecond continuum as a source of probe pulses was also applied to study the excitation decay dynamics in PBZT—a conjugated rigid-rod aromatic polymer with promising nonlinear optical and luminescent properties. The optical absorption in PBZT rises sharply at 500 nm, so frequency-doubled pulses (405 nm) from a Ti:sapphire amplifier were used to resonantly excite the PBZT sample. Using the white-light continuum generator, the photo-induced absorption was probed over a wide spectral range (from 500 to 1000 nm) below the PBZT bandgap. A broad photoinduced absorption band was observed: the signal appeared promptly within the time resolution and decayed in several picoseconds. The experimental results are explained by a self-trapped exciton model: induced absorption is due to the transition of self-trapped excitons to higher-lying continuum states. These results provide important information for the potential nonlinear optical and light-emitting applications of PBZT.

Test pump-probe experiments were performed in the mid-infrared range using the output of the optical parametric amplifier and difference frequency generator. In one set of measurements, a semiconductor sample (InGaAs ternary compound) was excited with the OPA output at 1.4 μm , and the DFG output was used as a probe. Photoinduced absorption due to free carriers was observed at a probe wavelength of 5 μm . In another experiment, the mid-infrared output of the difference frequency generator was utilized to monitor the intersubband-hole relaxation in quantum wells (InGaAs/AlGaAs heterostructure). These measurements were performed in the degenerate pump-probe configuration at the 5- μm wavelength, resonant with the intersubband (heavy-hole to light-hole) transition. An increase of transmission (bleaching) following photoexcitation was observed (Fig. 65.49). The bleaching signal recovered with a time constant of about 0.6 ps, corresponding to the excited state (light-hole subband) lifetime.

Conclusions

An ultrafast Ti:sapphire laser/amplifier system has been developed and characterized. Its output has been used to produce tunable femtosecond pulses in the near- and mid-infrared range using white-light continuum generation, optical parametric amplification, and difference frequency mixing. Although further optimization of the nonlinear optical fre-



Z2108

Figure 65.49 Pump-probe bleaching signal of a quantum well sample. The cross-correlation of the pump and probe pulses is shown for comparison (thin line).

quency converters is needed, the system is already capable of ultrafast optical experiments in the infrared range. Initial ultrafast spectroscopic experiments have been performed on a number of materials, important for both scientific and technological studies.

ACKNOWLEDGMENT

This work was supported by the National Science Foundation (Grant No. ECS-9413989).

REFERENCES

1. J. D. Kafka, M. L. Watts, and J.-W. J. Pieterse, *IEEE J. Quantum Electron.* **28**, 2151 (1992).
2. P. Maine, D. Strickland, P. Bado, M. Pessot, and G. Mourou, *IEEE J. Quantum Electron.* **24**, 398 (1988).
3. R. L. Fork *et al.*, *Opt. Lett.* **8**, 1 (1983).
4. For a recent review of results on optical parametric amplification see *J. Opt. Soc. Am. B* **12**, 1995 (special issue on optical parametric devices).
5. V. G. Dmitriev, G. G. Gurzadyan, D. N. Nikogosyan, *Handbook of Nonlinear Optical Crystals* (Springer-Verlag, Berlin, 1991), p. 78.
6. D. You *et al.*, *Opt. Lett.* **18**, 290 (1993).
7. J. T. Darrow *et al.*, *Opt. Lett.* **15**, 323 (1990).
8. R. R. Jones, D. You, and P. H. Bucksbaum, *Phys. Rev. Lett.* **70**, 1236 (1993).
9. B. I. Greene *et al.*, *Appl. Phys. Lett.* **59**, 893 (1991).
10. S. Alexandrou, R. Sobelevski, and T. Y. Hsiang, *IEEE J. Quantum Electron.* **28**, 2325 (1992).

11. Z. D. Gaeta, M. W. Noel, and C. R. Stroud, Jr., *Phys. Rev. Lett.* **73**, 636 (1994).
12. L. T. Canham, *Appl. Phys. Lett.* **57**, 1046 (1990).
13. Laboratory for Laser Energetics LLE Review **62**, NTIS document No. DOE/SF/19460-75, 1995 (unpublished), p. 77.
14. J. von Behren, Y. Kostoulas, K. B. Üçer, and P. M. Fauchet, to be published in the *Journal of Non-Crystalline Solids*.